THE JOURNAL OF BIOLOGICAL CHEMISTRY VOL. 286, NO. 21, pp. 19065–19075, May 27, 2011

Demonstration of Physical Proximity between the N Terminus and the S4-S5 Linker of the Human *ether-à-go-go*-related Gene (hERG) Potassium Channel*[S]

Received for publication, March 10, 2011, and in revised form, March 31, 2011 Published, JBC Papers in Press, April 7, 2011, DOI 10.1074/jbc.M111.238899

Pilar de la Peña[1], Carlos Alonso-Ron[2], Angeles Machín[3], Jorge Fernández-Trillo[4], Luis Carretero[4], Pedro Domínguez, and Francisco Barros

From the Department of Biochemistry and Molecular Biology, University of Oviedo, 33006 Oviedo, Spain

Potassium channels encoded by the human *ether-à-go-go*-related gene (hERG) contribute to cardiac repolarization as a result of their characteristic gating properties. The hERG channel N terminus acts as a crucial determinant in gating. It is also known that the S4-S5 linker couples the voltage-sensing machinery to the channel gate. Moreover, this linker has been repeatedly proposed as an interaction site for the distal portion of the N terminus controlling channel gating, but direct evidence for such an interaction is still lacking. In this study, we used disulfide bond formation between pairs of engineered cysteines to demonstrate the close proximity between the beginning of the N terminus and the S4-S5 linker. Currents from channels with introduced cysteines were rapidly and strongly attenuated by an oxidizing agent, this effect being maximal for cysteine pairs located around amino acids 3 and 542 of the hERG sequence. The state-dependent modification of the double-mutant channels, but not the single-cysteine mutants, and the ability to readily reverse modification with the reducing agent dithiothreitol indicate that a disulfide bond is formed under oxidizing conditions, locking the channels in a non-conducting state. We conclude that physical interactions between the N-terminal-most segment of the N terminus and the S4-S5 linker constitute an essential component of the hERG gating machinery, thus providing a molecular basis for previous data and indicating an important contribution of these cytoplasmic domains in controlling its unusual gating and hence determining its physiological role in setting the electrical behavior of cardiac and other cell types.

* This work was supported in part by Spanish Ministerio de Ciencia e Innovación (MICINN) Grant BFU2009-11262 and Spanish Ion Channel Initiative (SICI) Consolider-Ingenio Project CSD2008-00005.

[S] The on-line version of this article (available at http://www.jbc.org) contains supplemental Fig. 1.

[1] To whom correspondence should be addressed: Dept. de Bioquímica y Biología Molecular, Ed. Santiago Gascón, University of Oviedo, 33006 Oviedo, Spain. Tel.: 34-985-104-211; Fax: 34-985-103-157; E-mail: pdelapena@uniovi.es.

[2] Present address: Fundación de Investigación Oftalmológica, Instituto Oftalmológico Fernández-Vega, Avda Dres Fernández-Vega s/n., 33012 Oviedo, Asturias, Spain.

[3] Supported by a postdoctoral contract from Spanish Ion Channel Initiative Consolider 2008.

[4] Supported by predoctoral fellowships from the Ministerio de Educación y Ciencia (MEC) and the Fondo de Investigación Científica y Técnica (FICYT) of Spain.

ether-à-go-go-related gene potassium channels play a key role in setting the electrical behavior of a variety of cell types (Refs. 1–3 and references therein). Among other physiological functions, the human *ether-à-go-go*-related gene (hERG[5]; Kv11.1) channel mediates the cardiac repolarizing current (I_{Kr}) (4, 5). Malfunction of hERG due to either pharmacological block by medications or inherited mutations is a major cause of type 2 long-QT syndrome (4, 6–11), a disorder of ventricular repolarization that predisposes affected individuals to ventricular arrhythmia and sudden death (6, 12, 13). The various roles of hERG derive from its unusual gating properties, characterized by slow activation kinetics and a very fast inactivation on depolarization. On the other hand, during repolarization, hERG currents increase due to a fast recovery from inactivation followed by a much slower deactivation. This maintains the channels open during longer periods of time at negative voltages, giving rise to the typical hERG tail currents. In the case of the heart, this contributes to the repolarization of the cardiac action potential and to the prevention of arrhythmias induced by early after-depolarizations or ectopic beats (14, 15).

As for other voltage-dependent potassium channels, the main components of the hERG gating machinery (*e.g.* the voltage-sensing structures and the gate) are located in the transmembrane channel core (16–23). However, it has been demonstrated that the distinctive gating properties of hERG are strongly influenced by other cytoplasmic protein domains. Thus, the important role of the distal *eag*/PAS and exclusive proximal domains of the N terminus in the activation properties and their modulation by hormones has been demonstrated (1, 2, 23–26). It is known that the initial region of hERG N terminus determines its slow deactivation, whereas the proximal domain is the functionally critical region for slowing activation gating (24, 27–33). Also, it has recently been proposed that some residues in the N-terminal portions of the C terminus (either in the named "C-linker" between the last transmembrane segment (S6) and the cyclic nucleotide-binding domain (cNBD) homologous region or in the cNBD itself) could be involved in the control of deactivation gating, possibly through their interaction with the N-terminal-most initial regions of the N terminus (34–36).

Whereas the involvement of the hERG N terminus in the regulation of activation and deactivation gating is largely rec-

[5] The abbreviations used are: hERG, human *ether-à-go-go*-related gene; cNBD, cyclic nucleotide-binding domain; $TbHO_2$, *tert*-butyl hydroperoxide.

ognized, the molecular basis of this effect is not totally understood. It has been repeatedly proposed that an interaction between N-terminal domains and the S4-S5 linker is the cause of the strong influence exerted by the N terminus in the gating properties (1, 16, 23–25, 27–33, 37–39). Nevertheless, evidence for this interpretation is mostly indirect, including (i) the essential role of the S4-S5 linker coupling voltage sensor activation to the activation gate (38, 40), (ii) the strong parallelism between the alterations in gating caused by mutations in the N terminus and those in the S4-S5 linker (1, 16, 24, 27–33, 37, 41), (iii) the prevention of deactivation slowing by the N terminus after mutation of Gly-546 in the S4-S5 linker to cysteine and its subsequent modification by the addition of the sulfhydryl reagent *N*-ethylmaleimide (29), (iv) the impairment of the cytoplasmic domain-dependent modulation of gating in response to hormonal treatments by single-point mutations in the initial portion of the S4-S5 linker (2), (v) the restoration of slow deactivation gating by the addition of synthetic or recombinant N-terminal domains to channels lacking the N terminus (28, 31, 32), and (vi) the closer positioning of the N-terminal-most segments of the hERG N terminus toward the transmembrane channel core structures compared with other cytoplasmic regions of the channel (3). Note, however, that despite these findings, a direct demonstration of a physical interaction between the distal portion of the N terminus and the S4-S5 linker in the entire channel protein is lacking. Binding of a nonapeptide derived from the S4-S5 linker to the *eag*/PAS domain has been recently reported by NMR titration studies (39). However, in this case, only isolated protein fragments were used, and the peptide specificity of the results was not checked. Therefore, the possibility that the modulation of gating is due to a distant allosteric interaction between these domains cannot be excluded, and the specific details of the putative binding site remain to be determined.

In this study, we used a site-directed cysteine and disulfide chemistry approach (42) to form disulfide cross-links between pairs of introduced cysteines at the beginning of the N terminus and in the S4-S5 linker. Because application of a short peptide corresponding to the first 16 amino acids of hERG is able to restore slow deactivation gating of N-terminally truncated channels (31), and short deletions in the flexible portion at the beginning of the N terminus reproduce the effects on deactivation gating of more extensive N-terminal deletions (29, 31, 33), also mimicking the effect of mutations in the N-terminal portion of the S4-S5 linker (1, 29, 37), we concentrated our work in these regions. Disulfide bonding was detected by measuring the selective, state-dependent, and DTT-reversible elimination of the double-mutant currents under oxidizing conditions, thus demonstrating the proximity between these domains in fully functional channels present on the cell surface.

EXPERIMENTAL PROCEDURES

Reagents and Molecular Biology—The oxidizing agent *tert*-butyl hydroperoxide ($TbHO_2$; Sigma) was diluted in bath solution shortly before experiments. DTT (Sigma and Fluka) was dissolved in the experimental medium immediately before use.

Site-directed mutagenesis using the PCR-based overlap extension method, *in vitro* synthesis of cRNA, and injection of cRNA into *Xenopus laevis* oocytes were performed as described previously (1, 2). Oocytes were injected and incubated in OR-2 medium (82.5 mM NaCl, 2 mM KCl, 2 mM $CaCl_2$, 2 mM $MgCl_2$, 1 mM Na_2PO_4, and 10 mM HEPES, pH 7.4) for 2–3 days as described (1, 2).

Electrophysiology—hERG currents were measured in manually defolliculated oocytes with the two-electrode voltage-clamp method as described previously (1, 2, 24, 26). Unless stated otherwise, recordings were obtained in OR-2 medium. Exceptionally (*e.g.* for the P2C/Y542C construct) high-K^+ OR-2 medium in which 50 mM KCl replaced an equivalent amount of NaCl was used to maximize currents of those constructs showing a low level of functional expression. Parallel experiments with several single- and double-cysteine mutants indicated that the extent and kinetics of the oxidation and reduction effects were the same in both solutions. Membrane potential was typically clamped at −80 mV. Where indicated, a holding potential of +40 mV was used to maintain the channels open/inactivated during the oxidation treatments. Ionic currents sampled at 1 kHz were elicited using the voltage protocols indicated in the figures. To prevent any influence of the oxidizing and reducing agents on the silver chloride ground electrodes, they were connected to the bath chamber through agar bridges. Stimulation and data acquisition were controlled with Pulse+PulseFit software (HEKA Elektronik, Lambrecht, Germany) running on Macintosh computers.

Data Analysis—Data analysis and exponential fits to ionic currents and time courses were performed with the programs PulseFit (HEKA Elektronik) and Igor-Pro (WaveMetrics, Lake Oswego, OR). Current kinetic parameters were obtained as described previously (1, 2, 24, 26).

Data values given in the text and in the figures with *error bars* represent the mean ± S.E. for the number of indicated cells. Comparisons between data groups were at first performed by parametric Student's impaired *t* test (two-tailed). When significant differences in S.D. were present, an alternate Welch's test or non-parametric Wilcoxon or Mann-Whitney test was also used. In all cases, p values <0.05 were considered as indicative of statistical significance.

RESULTS AND DISCUSSION

Effect of Oxidation-Reduction on Single- and Double-cysteine hERG Mutants in the N Terminus and the S4-S5 Linker—The existence of an interaction between the N-terminal domains and the S4-S5 linker of hERG has been repeatedly related to modulation of activation and deactivation gating by the N terminus (1, 16, 23–25, 27–33, 37–39). However, apart from indirect evidence provided mainly by the similar deactivation properties caused by structural modifications in both domains (1–3, 16, 24, 27–33, 37, 38, 40, 41), direct proof of such an interaction is still lacking. Site-directed cysteine and disulfide chemistry can be used to map out contacts between pairs of positions or to demonstrate the physical proximity between protein sequences carrying the pair of introduced cysteines (42). Therefore, we introduced cysteines into specific positions of the distal portion of the hERG N terminus and the S4-S5 linker, either singly or simultaneously, and then applied the membrane-permeable oxidizing agent $TbHO_2$ to oocytes expressing the constructs to

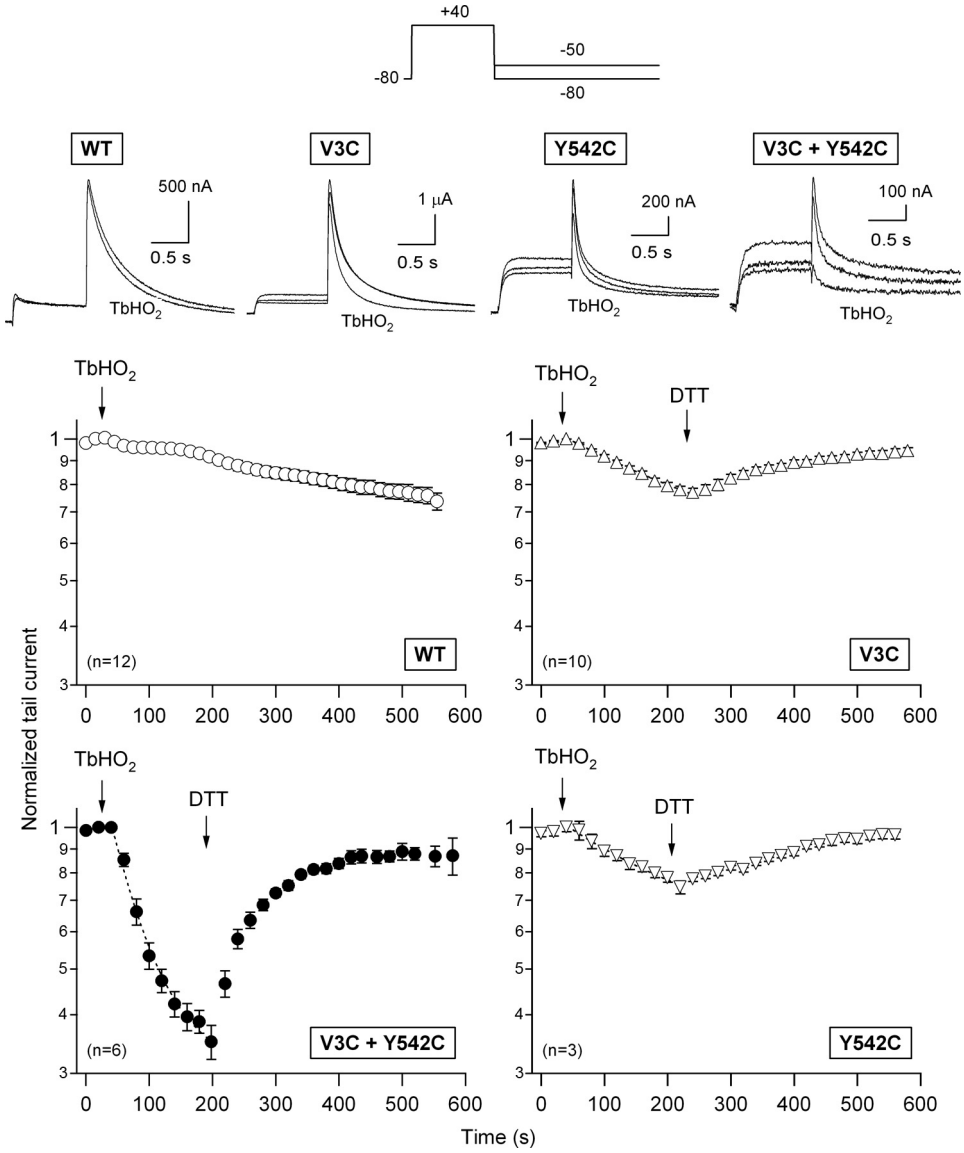

FIGURE 1. **Effect of extracellularly applied $TbHO_2$ and DTT on hERG currents.** The pulse protocol used to activate/inactivate and deactivate hERG channels expressed in *Xenopus* oocytes is shown at the top. Tail currents were recorded during repolarizations to −80 mV (WT) or −50 mV (mutants) to compensate for the faster deactivation of the N-terminal and S4-S5 linker mutants. These repolarizations followed 1-s depolarizing steps to +40 mV from a holding potential of −80 mV. Following stabilization of the tail currents, 2 mM $TbHO_2$ and 5 mM DTT were applied as indicated. The time course of peak tail current variation was followed for ~10 min. Data corresponding to channels carrying single-cysteine substitutions at residues 3 and 542 of the hERG sequence and to the double-cysteine mutant V3C/Y542C are illustrated in the graphs. Data points represent the mean ± S.E. of current magnitudes normalized to the value obtained immediately before $TbHO_2$ addition. Monoexponential fits are shown superimposed on the data during the $TbHO_2$ treatment. Superposition of two (WT) or three (mutants) current sweeps before, 3 min after application of $TbHO_2$, and 5 min after the addition of DTT are shown in the *insets*. The *lower trace* always corresponds to $TbHO_2$ treatment.

study the effects of redox-dependent disulfide bonding between the respective cysteines.

The hERG sequence contains 24 endogenous cysteines. Ten of them are located in the *eag*/PAS (eight cysteines) and proximal (two cysteines) domains of the N terminus. Two cysteines are in the extracellular S1-S2 linker, and three are in the S5 and S6 transmembrane helices. The remaining nine cysteines are in the C terminus: four in the C-linker, one in the cNBD, and four in the distal half of the C terminus. However, at least under the experimental conditions used here, these native cysteines are functionally "silent" because the WT hERG currents decreased only minimally and very slowly following treatment with $TbHO_2$ (Fig. 1). The activation and deactivation properties of the WT channels were not appreciably altered by oxidation (data not shown) (43, 44). Introduction of a single-cysteine residue at the beginning of the N terminus (*e.g.* in mutant V3C; see also below) slightly but consistently increased the $TbHO_2$-induced inhibition of the hERG tail current (from a normalized I_{tail} decrease of 5.9 ± 1.5% ($n = 12$) in the WT to 21.2 ± 1.6% ($n = 10$) in V3C channels following a 3-min $TbHO_2$ treatment; $p < 0.001$). A similar effect was obtained in response to $TbHO_2$ when a single cysteine was introduced into the N-terminal portion of the S4-S5 linker (mutant Y542C) (Fig. 1). In this case, the tail current was reduced by 25.4 ± 3.0% ($n = 3$; $p < 0.001$ *versus* the WT). The evolution of these effects was slow, with estimated time constants of 318 ± 22 and 220 ± 44 s for the V3C

and Y542C channels, respectively. By contrast, the current mediated by a construct carrying two engineered cysteines at Val-3 and Tyr-542 (double mutant V3C/Y542C) (Fig. 1) was rapidly and strongly reduced by $TbHO_2$. Thus, an inhibition time constant of 57.5 ± 2.8 s ($n = 6$) was observed, and the I_{tail} decrease amounted to 65 ± 2.9% following a 3-min treatment ($p < 0.001$ *versus* the WT, V3C, and Y542C alone). Noticeably, the kinetic properties of the small residual currents after oxidation closely resemble those of the original ones before adding the oxidizing agent (supplemental Fig. 1). Therefore, the observed reductions are not due to a kinetic shift that minimizes the size of the currents exclusively at the potentials used for the measurements. Even though other mechanistic interpretations could be possible (*e.g.* that oxidation-induced modifications of V3C and Y542C synergistically interact), these results clearly suggest that disulfide bonding between Cys-3 and Cys-542 occurs, thus compromising activation gating and locking a substantial fraction of channels in a non-conducting state.

If the diminished opening of the oxidized double-cysteine mutant resulted from formation of a disulfide bond, then the effect should be readily reversible by application of DTT, a reducing agent whose only action should be to break disulfide bonds (40, 43–45). Changing to normal extracellular solution following the treatment with $TbHO_2$ did not appreciably reverse the inhibitory effect of the oxidizing agent (data not shown). Also, no measurable effects of DTT were observed when the reducing agent was directly applied to oocytes expressing either the WT or double-mutant channels (data not shown), indicating that disulfide bonds were not present under control conditions, perhaps due to the reducing environment of the oocyte interior. However, as shown in Fig. 1, the $TbHO_2$-induced reduction of the V3C/Y542C current was rapidly (recovery time constant of 75.2 ± 7.3 s) and almost completely reversed when 5 mM DTT was substituted for the oxidizing agent in the external medium. Thus, a steady-state current level amounting to 83 ± 8% of the initial control value was attained in the presence of the reducing agent. This also suggests that the effect of the oxidizing agent was not due to a nonspecific disruption of the cell integrity.

It is interesting to note that we were unable to observe any consistent pattern of DTT effects on the otherwise very small response to $TbHO_2$ of the WT-expressing oocytes (data not shown). However, the addition of the reducing agent reversed the effect caused by the oxidation of the V3C (75 ± 7% reversal) and Y542C (84 ± 8% reversal) mutant channels (Fig. 1). Even though the kinetics of this reversion were markedly slower than those observed with the double-mutant construct (recovery time constants of 172 ± 6 and 500 ± 198 s for the V3C and Y542C channels, respectively; $p < 0.001$), these data raised the possibility that, albeit with smaller effectivity and/or reduced functional impact, a disulfide bond could also be forming between the cysteines at these positions and an endogenous cysteine in the channel. Unfortunately, both a multiple mutant without any native cysteine in the N terminus and an hERG construct lacking extensive regions of the C terminus yielded electrophysiologically non-functional channels (see also Ref. 35). Therefore, we generated a battery of single- and double-point mutants from which most of the endogenous cysteines present in the intracellular domains of hERG were removed and combined them with the V3C mutation. The effect caused by $TbHO_2$-induced oxidation of these constructs is summarized in Fig. 2.

It has been recently shown that the cysteines located at positions 723 and 740 of the C-linker between the pore domain and the cytoplasmic cNBD are important for hERG function alterations caused by oxidative stress in HEK293 cells expressing the channel (35). We checked the possible implication of these residues in the slight inhibition induced by $TbHO_2$ in the single-point mutants (*e.g.* V3C) under our experimental conditions, also trying to minimize the possible contribution of these endogenous cysteines to the oxidation effect. For this purpose, we initially used two triple mutants carrying the V3C mutation but also lacking the endogenous cysteines at either positions 723 and 729 or positions 740 and 750. As shown in Fig. 2 (*A–C*), the small current inhibition elicited by the oxidizing agent in the V3C construct remained almost unaltered in mutants V3C/C723G/C729G and V3C/C740G/C750G.

In an additional set of experiments, oxidation of oocytes expressing quadruple mutants with two engineered cysteines at positions 3 and 542 but also with Cys-723 and Cys-729 or Cys-740 and Cys-750 changed to glycine (mutants V3C/Y542C/C723G/C729G and V3C/Y542C/C740G/C750G) rapidly and markedly lowered the current level. Thus, the level of inhibition and the inhibition time constant amounted to 76.8 ± 2.0% and 62.5 ± 5.6 s for the V3C/Y542C/C723G/C729G channels ($n = 4$; $p < 0.05$). These values corresponded to 69.9 ± 1.9% and 60 ± 9.7 s for V3C/Y542C/C740G/C750G ($n = 3$). Also, DTT largely reversed the oxidation effect in these constructs (91 ± 3.3 and 78 ± 2.1%, respectively). This reversion was also fast, with measured recovery time constants of 81.2 ± 11.0 and 83.3 ± 4.6 s, respectively. The reason for the slightly increased current attenuation by oxidation of channels carrying Cys-3 and Cys-542 but also lacking Cys-723 and Cys-729 is not known. It is possible that Cys-723 and Cys-729 are located near residues 3 and 542 in the channel structure, providing a competing environment for faster and more complete formation of disulfide products between Cys-3 and Cys-542 in the V3C/Y542C mutant (42).

Altogether, these data indicate that if Cys-3 establishes a cross-link with an endogenous cysteine, it is not any of the C-linker cysteines located at positions 723, 729, 740, and 750. They also demonstrate that for the prominent redox effects observed in the double mutant V3C/Y542C, these endogenous C-linker cysteines are not necessary.

In an additional attempt to analyze the reduced effect of $TbHO_2$ on the single-cysteine mutant V3C, we also combined it with a C-terminal deletion (mutant V3CΔ864–1010) in which elimination of residues 863 and 1011 removed the cysteines at positions 977 and 984 of the hERG sequence. This deletion did not appreciably modify the expression or electrophysiological properties of the channel (data not shown). An effect similar to that obtained with the V3C mutant was observed after the addition of $TbHO_2$ to the V3CΔ864–1010 construct (Fig. 2, *A* and *D*).

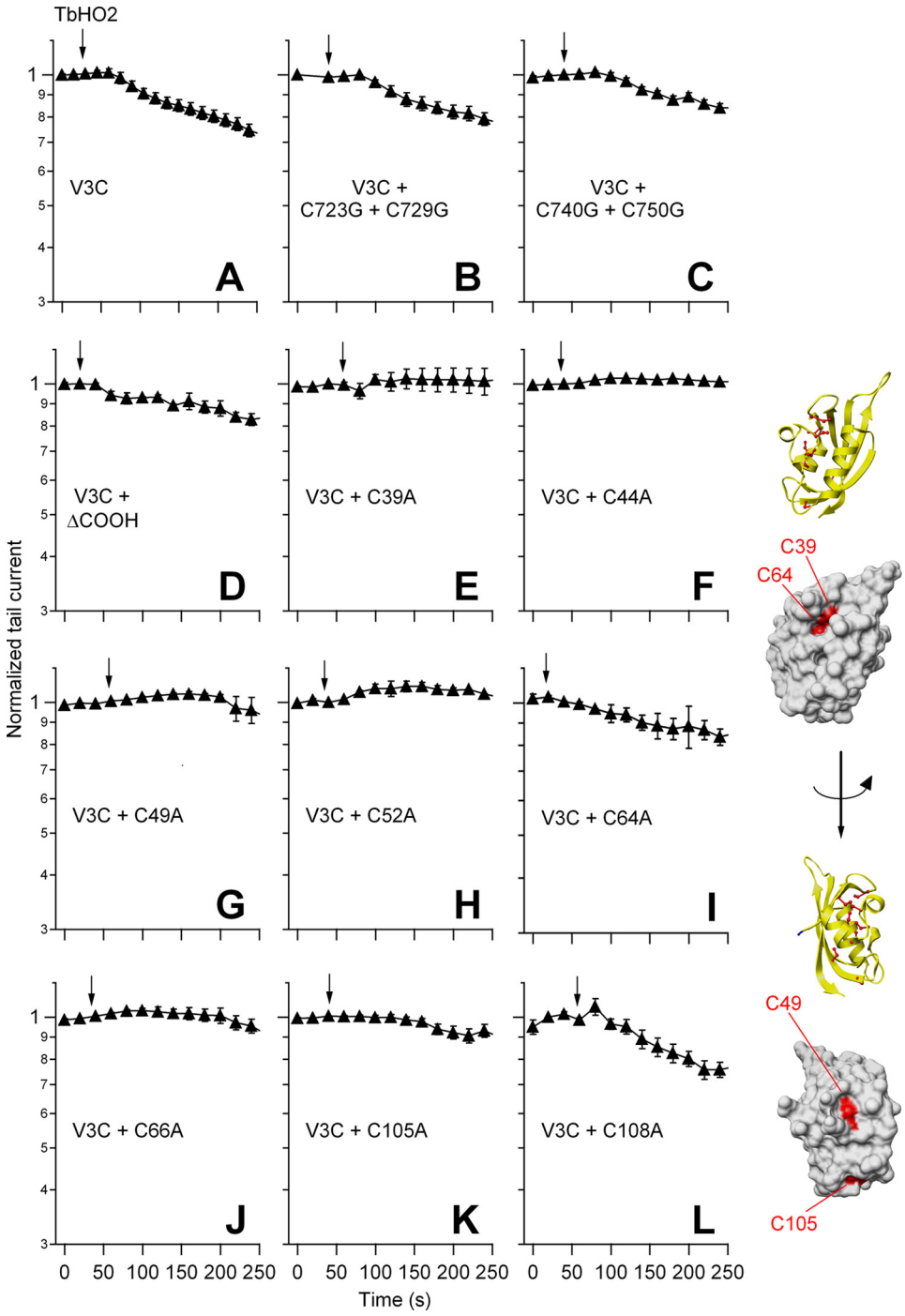

FIGURE 2. **Effect of $TbHO_2$ on V3C mutant channels in the presence or absence of endogenous cysteine residues.** The time course of normalized peak tail current variation after perfusion of 2 mM $TbHO_2$ (*arrows*) is shown. The identity of the single-, double-, and triple-mutant channel constructs is indicated in *A–C* and *E–L*. Data corresponding to a construct in which mutation V3C was combined with a C-terminal deletion removing residues 864–1010 (V3CΔCOOH) are shown in *D*. Averaged data from 5–10 oocytes are shown. Ribbon and surface representations of a single hERG *eag*/PAS domain corresponding to the x-ray tridimensional structure from Morais Cabral *et al.* (28) are shown on the *right*. The eight cysteines present in this channel region are shown in ball-and-stick representation in the ribbon diagrams. The positions of the four cysteine side chains (residues 39, 49, 64, and 105) that show up on the surface of the domain are highlighted in *red*. Note that the initial 26 residues of the hERG sequence not ordered in the crystal structure do not appear in the diagrams. Molecular graphic images were produced using the UCSF Chimera package from the Resource for Biocomputing, Visualization, and Informatics at the University of California, San Francisco.

Finally, we also created a set of double mutants in which the cysteine at position 3 was combined with a Cys-to-Ala mutation of every single cysteine of the *eag*/PAS domain. As shown in Fig. 2 (*E–L*), the absence of a cysteine at position 39, 44, 49, 52, 66, or 105 caused a reduction of the $TbHO_2$-induced current inhibition compared with that observed in the single mutant V3C. However, an effect of the oxidizing agent equivalent to that in the V3C mutant was obtained for the V3C/C64A and V3C/C108A mutants. The fact that elimination of several of the *eag*/PAS endogenous cysteines minimized the oxidation

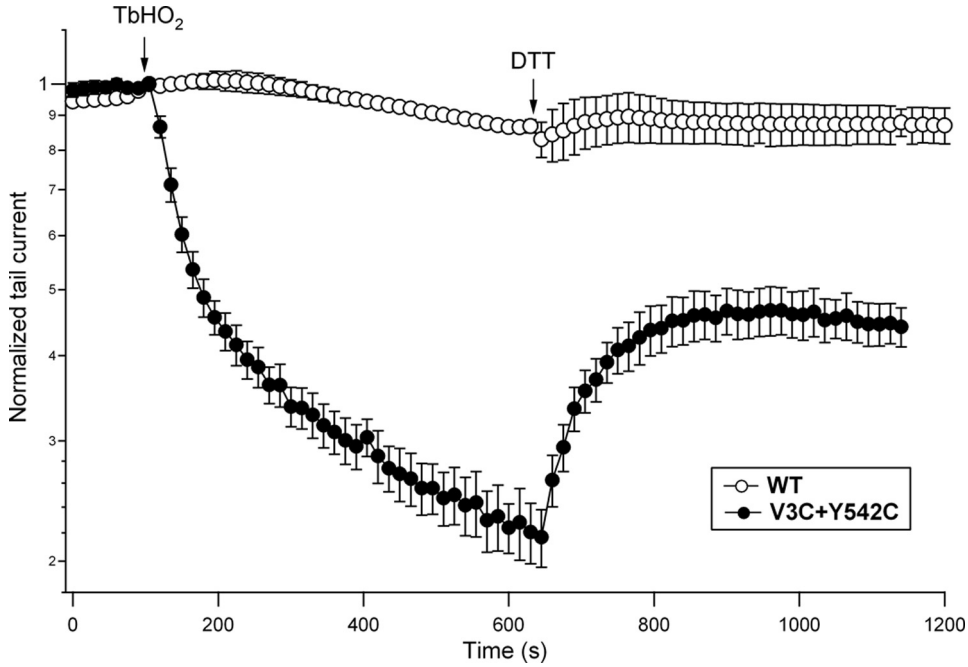

FIGURE 3. **Long-term evolution of the redox effects on hERG currents.** Peak tail currents were recorded from oocytes expressing WT (○) and V3C/Y542C (●) channels as described in the legend to Fig. 1. An extended treatment of ~10 min with 2 mM $TbHO_2$ was performed, followed by a period of perfusion without the oxidizing agent in which 20 mM DTT was substituted for 10 mM NaCl in OR-2 medium. Averaged data from four oocytes are shown.

effect on V3C channels could be interpreted as an indication that some interaction takes place between residues at these positions and the cysteine at position 3. However, similar results were observed upon thiol removal from amino acids such as Cys-39, Cys-49, and Cys-105 carrying side chains exposed to the surface of the *eag*/PAS crystalline structure (Fig. 2, *inset*) and from Cys-44, Cys-52, and Cys-66, localized in the domain core. Also, no change of the oxidizing agent effect was attained in mutants V3C/C64A and V3C/ C108A, even though Cys-64 and Cys-108 are indeed located in the periphery of the *eag*/PAS domain. Thus, it is likely that the effect of *eag*/PAS cysteine substitutions is indirectly due to a modification of the domain architecture and not to rupture of a disulfide bond between them and the cysteine introduced at position 3. Therefore, we next concentrated our efforts in further exploring the disulfide bond-related consequences of oxidation using double-cysteine mutants in both the N-terminal region and the S4-S5 linker.

Specificity of the Oxidation Effects—Careful inspection of the V3C/Y542C current attenuation after $TbHO_2$ addition indicated an apparent slowing of current inhibition at the latter time points of the $TbHO_2$ treatment (Fig. 1). Prolongation of the oxidizing agent treatment to 10 min more clearly revealed the slowed second phase of the $TbHO_2$ effect (Fig. 3). However, the enhancement of current inhibition was paralleled by a subsequent decrease in the fraction of current that could be recovered by the addition of DTT, even at the highest concentration used (20 mM). This indicates that non-disulfide products (*e.g.* sulfinic and sulfenic oxyacids) due to slower and DTT-irreversible oxidative reactions (42) can also accumulate after these long $TbHO_2$ treatments. Therefore, quantification of the oxidizing agent effects was systematically performed after 2–3-min treatments, followed by a phase of reversion with DTT.

One remarkable property of the disulfide chemistry approach is its dependence on the spatial proximity between the disulfide-forming pairs of residues. Besides variations due to structural fluctuations in separated but particularly flexible protein segments, rapid and extensive reactivity of cysteine pairs can be used as a good signature of such proximity (42). As a corollary, differences in the rate, extent, and reversal of the disulfide bond-forming reactions due to variations in the cysteine pairs can be used as an indication of specificity, particularly for adjacent positions of the same protein region. Oxidation of single-cysteine mutants at positions 4, 5, 6, and 8 of the N terminus yielded results analogous to those obtained with the single V3C mutant. Almost no effect of the oxidizing agent was observed with the S4-S5 single-cysteine mutant G546C (data not shown). Therefore, we tested the influence of changing the position of the cysteine pairs by modifying the locations of the cysteines both in the N terminus and in the S4-S5 linker.

The extent of the $TbHO_2$-induced inhibition of the hERG currents was maximal for cysteine pairs at position 3 or 4 of the N-terminal region and position 542 of the S4-S5 linker (Fig. 4). When the Cys-542 mutation was combined with a second cysteine at position 2, 5, 6, or 8 of the N terminus, the current inhibition was substantially reduced. Thus, only half of the attenuation of the double mutants V3C/Y542C and R4C/ Y542C was observed with respect to the single mutations V3C and Y542C (Fig. 5). A similarly small current inhibition was observed when the cysteine at position 3 was combined with a cysteine at position 545 of the S4-S5 linker. Furthermore, the $TbHO_2$-induced current attenuation was virtually abolished in the double mutant V3C/G546C. Noticeably, the double mutants carrying cysteine pairs at position 3 or 4 and position 542 also showed maximal speed of inhibition, which was followed by a faster and almost complete reversal upon DTT addition.

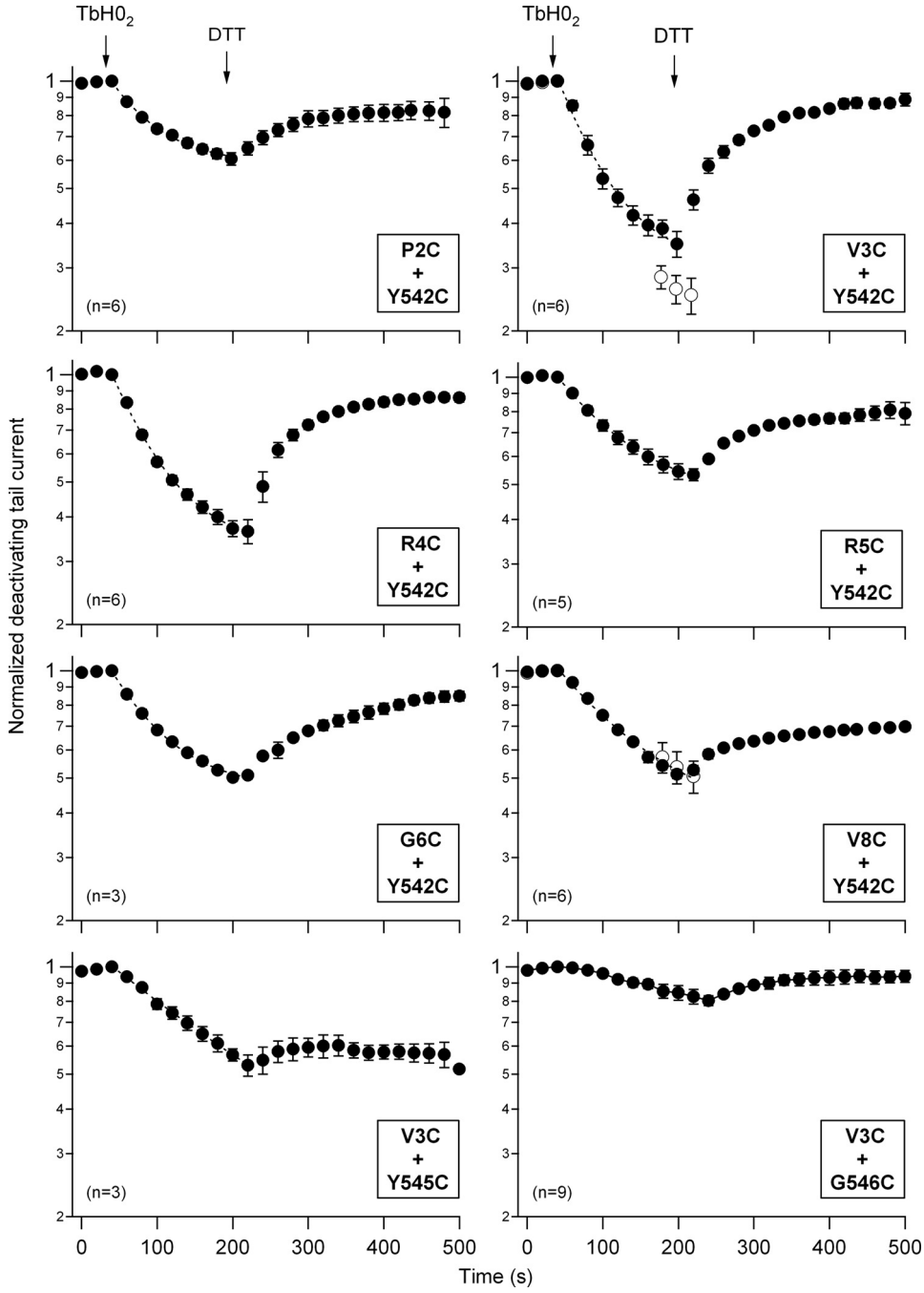

FIGURE 4. **Specificity of the redox effects as a function of the location of double-cysteine mutations.** The time course of the hERG current tail variations was followed upon the addition of 2 mM $TbHO_2$ and 5 mM DTT as indicated. Oocytes were bathed in standard OR-2 medium, except for the P2C/Y542C mutant, for which high-K^+ OR-2 medium (see "Experimental Procedures") was used because of the low expression level of this construct. Monoexponential fits are shown superimposed on the data during the $TbHO_2$ treatment. ○ (panels corresponding to mutants V3C/Y542C and V8C/Y542C), current level in a second set of oocytes following an oxidation period of 3 min in which test pulses were not applied to follow the evolution of the currents.

These kinetic parameters were substantially reduced either by changing the cysteine introduced into the N-terminal region at the beginning of the N terminus at position 2, 5, 6, and 8 or by using a combination of cysteine at position 3 with cysteines at positions 545 and 546. Altogether, these data further indicate that the oxidation effect leading to disulfide bond formation is maximal for those cysteine pairs located around amino acid 3 of the N terminus and amino acid 542 of the S4-S5 linker in the hERG sequence.

State Dependence of the Oxidation Effects—As a last indication of specificity and strong spatial dependence of the oxidation effects, we studied the state dependence of the current reductions induced by $TbHO_2$. The amount of the $TbHO_2$-induced V3C/Y542C current inhibition was significantly enhanced after 2–3 min of treatment when cells maintained at a holding potential of −80 mV were not repeatedly depolarized with the pulses to +40 mV used to analyze the time course of the oxidation effects (Fig. 4). This suggests that conformational

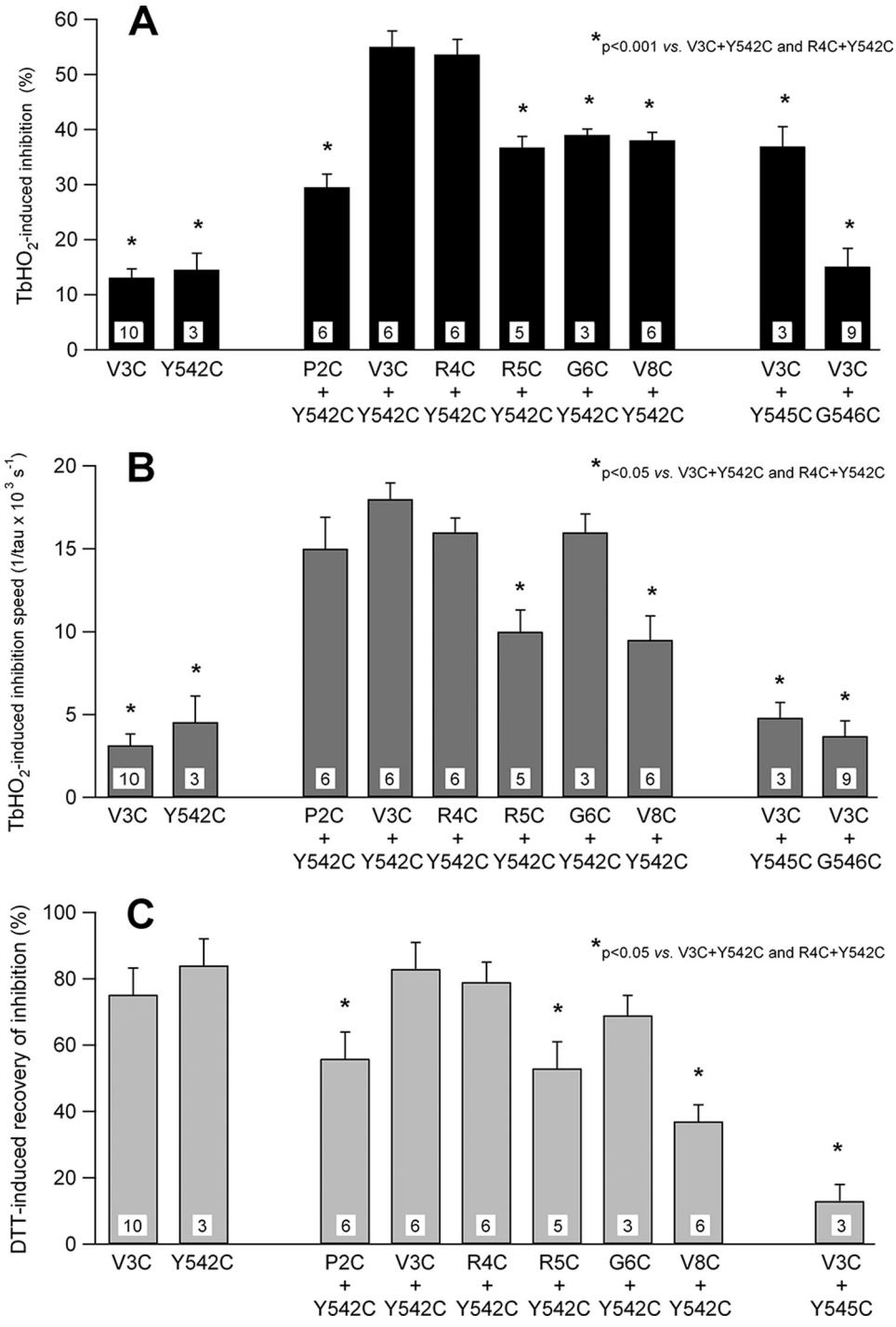

FIGURE 5. **Summary of the $TbHO_2$- and DTT-induced effects on hERG tail currents.** *A*, quantification of the $TbHO_2$-induced inhibition following a 3-min treatment with the oxidizing agent. The 5.9% inhibition measured in the non-mutated WT channels has been subtracted from the data. *B*, comparison of $TbHO_2$-induced inhibition rates. The speed of inhibition of the different constructs is compared as measured by the inverse value of the time constant obtained from monoexponential fits to the inhibitory phase upon the addition of $TbHO_2$. *C*, reversibility of the oxidation effect in the presence of DTT.

rearrangements during closed-to-open transitions are not essential for disulfide bond formation. Such enhancement was not observed with the V8C/Y542C pair. By contrast, holding the cell at +40 mV during the application of the oxidizing agent, therefore maintaining the channels in the open/inactivated state, markedly reduced the $TbHO_2$-induced inhibition of the V3C/Y542C currents (Fig. 6). This reduction was even more prominent when the V3C/Y542C channels were continuously maintained in the open/inactivated state at +40 mV during $TbHO_2$ treatment without repeatedly applying the hyperpolarizations used to follow the temporal evolution of the tail currents. Finally, no differences in the oxidation effects were observed when cells expressing the double-cysteine mutant G6C/Y542C were held at −80 mV (closed) or +40 mV (open/inactivated) during the application of $TbHO_2$.

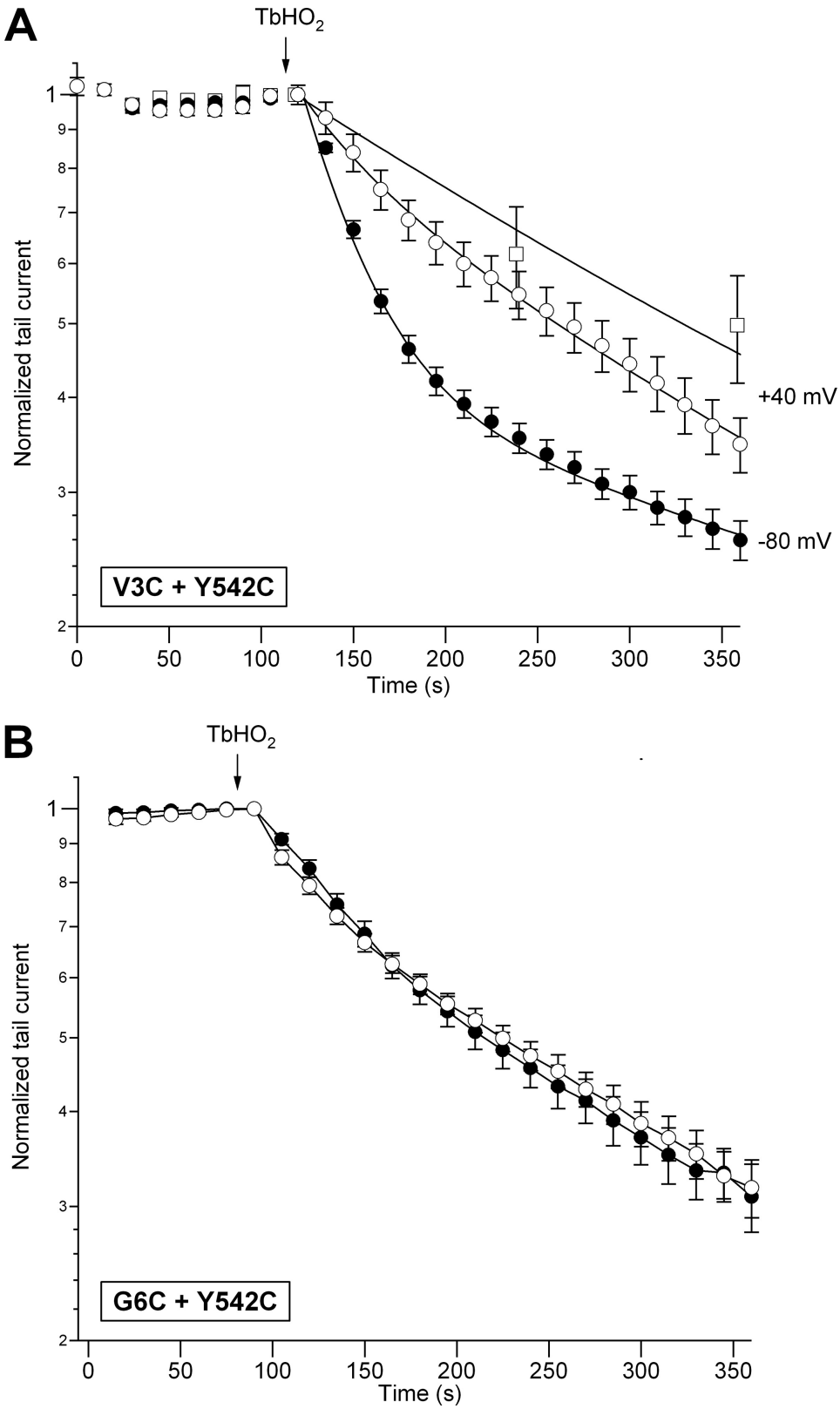

FIGURE 6. **State dependence of the $TbHO_2$-induced effect.** *A*, time course of V3C/Y542C peak tail current variation in response to $TbHO_2$. Peak tail currents were measured as described in the legend to Fig. 1 during repolarization steps applied at the indicated intervals from holding potentials of −80 mV (●) and +40 mV (○ and □). The magnitude of the peak tail currents was estimated at 15-s intervals (● and ○) or without continuous pulsing (□). The *continuous lines* correspond to exponential curves that best fit the data. Long treatments with the oxidizing agent were used to fit the data at +40 mV, but only data during the initial period of recording are shown for clarity. *B*, independence of the $TbHO_2$-induced effect on the conformational state of the G6C/Y542C channel. Channels were held closed at −80 mV (●) or open/inactivated at +40 mV (○) during the application of $TbHO_2$ as indicated in *A*. Note that, in this case, the inhibition kinetics superimpose onto the slow time course observed with V3C/Y542C channels held at +40 mV.

Formation of a disulfide bond requires close proximity between the sulfhydryl groups, meaning that cysteine residues separated by >7 Å would require motion of the protein backbone for disulfide cross-linkage (42, 46). However, it is difficult to translate our data to real distances because the probability of collision between the cysteine pairs forming disulfide bonds is greatly increased by fluctuations of otherwise flexible structures, even though they are located at a certain distance (40, 42, 45–47). There is evidence that the N-terminal-most segments of the hERG N terminus and the S4-S5 linker constitute highly flexible and/or unstructured regions (28, 33, 36, 39). The protein regions studied here are expected to be dynamically modulated during channel function, so it could be expected that collisions between the cysteine pairs may also be influenced by the molecular rearrangements associated with gating. Finally, some influence of the relatively slow permeation of redox reagents into the cells on the quantitative interpretation of our disulfide bond formation rates cannot be completely excluded.

The state-dependent modification of the V3C/Y542C mutant, but not the single-cysteine mutant channels, and the ability to readily reverse modification with the reducing agent DTT indicate that a disulfide bond is formed under oxidizing conditions between the N-terminal-most region of the N terminus and the S4-S5 linker, locking the channels in a non-conducting state. The covalent lock of the channels closed also indicates that the initial segment of the N terminus and the S4-S5 linker interact in the closed state. This would be consistent with our previous demonstration that the N-terminal-most region of the N terminus also plays a relevant role in activation properties (1). It would also be consistent with the reported ability of the Y542C mutation to positively shift the steady-state activation $V_{0.5}$ and its less negative ΔG_o, indicating a shift in the equilibrium toward the closed state (1).

It should be emphasized that our data do not exclude a contribution of other cytoplasmic structures (*e.g.* the PAS domain and the C-linker plus cNBD) to control gating via direct or indirect/allosteric interactions with the S4-S5 linker or other components of the gating machinery. Note that the most widely recognized effect of the N terminus is its contribution to slow deactivation gating, presumably also through an interaction with the S4-S5 linker that stabilizes the open state. Although we concentrated our efforts on the N-terminal segments or the N terminus and the S4-S5 linker, further work would be necessary to determine whether different regions of this linker (1, 2, 38, 48) and the structurally and functionally differentiated portions of the N terminus also contribute in specific ways to the protein-protein interactions that modulate gating. Note also that whereas an interaction of the S4-S5 linker with other gating components (*e.g.* the channel gate) seems to take place only in the closed state in hERG and KCNQ1 channels, the opposite happens in KAT1 and HCN channels, bearing a substantial homology to hERG in some cytoplasmic domains, and both open and closed state interactions take place between the same regions in *Shaker*-like potassium channels (49).

In this context, we propose that the physical interactions detected here between the N-terminal-most segments of the N terminus and the S4-S5 linker can be viewed as part of a global interaction network in which other cytoplasmic regions such as the PAS and proximal domains of the N terminus, the C-terminal portion of the sixth transmembrane segment, and the C-terminal C-linker and cNBD dynamically contribute to modulate channel gating. The functional consequence of these interactions on activation and deactivation and on inactivation gating (29, 50) can vary according to the channel type, the relative positioning of the N- and C-terminal portions, and the presence of additional auxiliary subunits.

In summary, our study provides, for the first time, direct evidence that a close proximity exists between the N-terminal-most region of the N terminus and the S4-S5 linker of hERG, which may allow for a physical interaction between these cytoplasmic domains. Therefore, it sheds significant new insight into the molecular basis of the protein-protein interactions between the N-terminal distal regions and the S4-S5 linker involved in the control of gating properties and hormonal modulation of hERG (1, 2, 24, 27–33, 36).

Acknowledgments—We thank Dr. Kevin Dalton for editing the manuscript. The Resource for Biocomputing, Visualization, and Informatics at the University of California, San Francisco, is supported by National Institutes of Health Grant P41 RR001081.

REFERENCES

1. Alonso-Ron, C., de la Peña, P., Miranda, P., Domínguez, P., and Barros, F. (2008) *Biophys. J.* **94,** 3893–3911
2. Alonso-Ron, C., Barros, F., Manso, D. G., Gómez-Varela, D., Miranda, P., Carretero, L., Domínguez, P., and de la Peña, P. (2009) *Pflügers Arch.* **457,** 1237–1252
3. Miranda, P., Manso, D. G., Barros, F., Carretero, L., Hughes, T. E., Alonso-Ron, C., Domínguez, P., and de la Peña, P. (2008) *Biochim. Biophys. Acta* **1783,** 1681–1699
4. Sanguinetti, M. C., Jiang, C., Curran, M. E., and Keating, M. T. (1995) *Cell* **81,** 299–307
5. Trudeau, M. C., Warmke, J. W., Ganetzky, B., and Robertson, G. A. (1995) *Science* **269,** 92–95
6. Viskin, S. (1999) *Lancet* **354,** 1625–1633
7. Chiang, C. E., and Roden, D. M. (2000) *J. Am. Coll. Cardiol.* **36,** 1–12
8. Keating, M. T., and Sanguinetti, M. C. (2001) *Cell* **104,** 569–580
9. Redfern, W. S., Carlsson, L., Davis, A. S., Lynch, W. G., MacKenzie, I., Palethorpe, S., Siegl, P. K., Strang, I., Sullivan, A. T., Wallis, R., Camm, A. J., and Hammond, T. G. (2003) *Cardiovasc. Res.* **58,** 32–45
10. Thomas, D., Zhang, W., Wu, K., Wimmer, A. B., Gut, B., Wendt-Nordahl, G., Kathöfer, S., Kreye, V. A., Katus, H. A., Schoels, W., Kiehn, J., and Karle, C. A. (2003) *Cardiovasc. Res.* **59,** 14–26
11. Finlayson, K., Witchel, H. J., McCulloch, J., and Sharkey, J. (2004) *Eur. J. Pharmacol.* **500,** 129–142
12. Roden, D. M., Lazzara, R., Rosen, M., Schwartz, P. J., Towbin, J., and Vincent, G. M. (1996) *Circulation* **94,** 1996–2012
13. Schwartz, P. J. (2005) *Nat. Clin. Pract. Cardiovasc. Med.* **2,** 346–351
14. Smith, P. L., Baukrowitz, T., and Yellen, G. (1996) *Nature* **379,** 833–836
15. Lu, Y., Mahaut-Smith, M. P., Varghese, A., Huang, C. L., Kemp, P. R., and Vandenberg, J. I. (2001) *J. Physiol.* **537,** 843–851
16. Liu, J., Zhang, M., Jiang, M., and Tseng, G. N. (2003) *J. Gen. Physiol.* **121,** 599–614
17. Subbiah, R. N., Clarke, C. E., Smith, D. J., Zhao, J., Campbell, T. J., and Vandenberg, J. I. (2004) *J. Physiol.* **558,** 417–431
18. Subbiah, R. N., Kondo, M., Campbell, T. J., and Vandenberg, J. I. (2005) *J. Physiol.* **569,** 367–379
19. Zhang, M., Liu, J., Jiang, M., Wu, D. M., Sonawane, K., Guy, H. R., and Tseng, G. N. (2005) *J. Membr. Biol.* **207,** 169–181
20. Smith, P. L., and Yellen, G. (2002) *J. Gen. Physiol.* **119,** 275–293
21. Piper, D. R., Varghese, A., Sanguinetti, M. C., and Tristani-Firouzi, M.

(2003) *Proc. Natl. Acad. Sci. U.S.A.* **100,** 10534–10539
22. Zhang, M., Liu, J., and Tseng, G. N. (2004) *J. Gen. Physiol.* **124,** 703–718
23. Saenen, J. B., Labro, A. J., Raes, A., and Snyders, D. J. (2006) *Biophys. J.* **91,** 4381–4391
24. Viloria, C. G., Barros, F., Giráldez, T., Gómez-Varela, D., and de la Peña, P. (2000) *Biophys. J.* **79,** 231–246
25. Gómez-Varela, D., de la Peña, P., García, J., Giráldez, T., and Barros, F. (2002) *J. Membr. Biol.* **187,** 117–133
26. Gómez-Varela, D., Barros, F., Viloria, C. G., Giráldez, T., Manso, D. G., Dupuy, S. G., Miranda, P., and de la Peña, P. (2003) *FEBS Lett.* **535,** 125–130
27. Spector, P. S., Curran, M. E., Zou, A., Keating, M. T., and Sanguinetti, M. C. (1996) *J. Gen. Physiol.* **107,** 611–619
28. Morais Cabral, J. H., Lee, A., Cohen, S. L., Chait, B. T., Li, M., and Mackinnon, R. (1998) *Cell* **95,** 649–655
29. Wang, J., Trudeau, M. C., Zappia, A. M., and Robertson, G. A. (1998) *J. Gen. Physiol.* **112,** 637–647
30. Chen, J., Zou, A., Splawski, I., Keating, M. T., and Sanguinetti, M. C. (1999) *J. Biol. Chem.* **274,** 10113–10118
31. Wang, J., Myers, C. D., and Robertson, G. A. (2000) *Biophys. J.* **115,** 749–758
32. Gustina, A. S., and Trudeau, M. C. (2009) *Proc. Natl. Acad. Sci. U.S.A.* **106,** 13082–13087
33. Ng, C. A., Hunter, M. J., Perry, M. D., Mobli, M., Ke, Y., Kuchel, P. W., King, G. F., Stock, D., and Vandenberg, J. I. (2011) *PLoS ONE* **6,** e16191
34. Al-Owais, M., Bracey, K., and Wray, D. (2009) *Eur. Biophys. J.* **38,** 569–576
35. Kolbe, K., Schönherr, R., Gessner, G., Sahoo, N., Hoshi, T., and Heinemann, S. H. (2010) *J. Physiol.* **588,** 2999–3009
36. Muskett, F. W., Thouta, S., Thomson, S. J., Bowen, A., Stansfeld, P. J., and Mitcheson, J. S. (2011) *J. Biol. Chem.* **286,** 6184–6191
37. Sanguinetti, M. C., and Xu, Q. P. (1999) *J. Physiol.* **514,** 667–675
38. Van Slyke, A. C., Rezazadeh, S., Snopkowski, M., Shi, P., Allard, C. R., and Claydon, T. W. (2010) *Biophys. J.* **99,** 2841–2852
39. Li, Q., Gayen, S., Chen, A. S., Huang, Q., Raida, M., and Kang, C. (2010) *Biochem. Biophys. Res. Commun.* **403,** 126–132
40. Ferrer, T., Rupp, J., Piper, D. R., and Tristani-Firouzi, M. (2006) *J. Biol. Chem.* **281,** 12858–12864
41. Schönherr, R., and Heinemann, S. H. (1996) *J. Physiol.* **493,** 635–642
42. Bass, R. B., Butler, S. L., Chervitz, S. A., Gloor, S. L., and Falke, J. J. (2007) *Methods Enzymol.* **423,** 25–51
43. Liu, J., Zhang, M., Jiang, M., and Tseng, G. N. (2002) *J. Gen. Physiol.* **120,** 723–737
44. Brown, S., Sonntag, D. P., and Sanguinetti, M. C. (2008) *Cell Physiol. Biochem.* **22,** 601–610
45. Bell, D. C., Turbendian, H. K., Valley, M. T., Zhou, L., Riley, J. H., Siegelbaum, S. A., and Tibbs, G. R. (2009) *Pflügers Arch.* **458,** 259–272
46. Falke, J. J., Dernburg, A. F., Sternberg, D. A., Zalkin, N., Milligan, D. L., and Koshland, D. E., Jr. (1988) *J. Biol. Chem.* **263,** 14850–14858
47. Horenstein, J., Wagner, D. A., Czajkowski, C., and Akabas, M. H. (2001) *Nat. Neurosci.* **4,** 477–485
48. Ju, P., Pages, G., Riek, R. P., Chen, P. C., Torres, A. M., Bansal, P. S., Kuyucak, S., Kuchel, P. W., and Vandenberg, J. I. (2009) *J. Biol. Chem.* **284,** 1000–1008
49. Choveau, F. S., Rodriguez, N., Ali, F. A., Labro, A. J., Rose, T., Dahimène, S., Boudin, H., Le Hénaff, C., Escande, D., Snyders, D. J., Charpentier, F., Mérot, J., Baró, I., and Loussouarn, G. (2011) *J. Biol. Chem.* **286,** 707–716
50. Barghaan, J., and Bähring, R. (2009) *J. Gen. Physiol.* **133,** 205–224